IMTC 2004 – Instrumentation and Measurement
Technology Conference
Como, Italy, 18-20 May 2004

Evaluation of Performance of Multi–Antenna Terminals Using Two Approaches

P. Suvikunnas[1], K. Sulonen[1], J. Villanen[1], C. Icheln[1], J. Ollikainen[2], P. Vainikainen[1]
[1]Radio Laboratory/SMARAD, Helsinki University of Technology
P. O. Box 3000, FI–02015 HUT, FINLAND
Phone: +358 9 451 2248, Fax: + 358 9 2152, Email: pasi.suvikunnas@hut.fi
[2]Nokia Research Center, P.O. Box 407, FI–00045 NOKIA GROUP, Finland

Abstract – *In this work, a novel and fast plane–wave based method for evaluation of multi–antenna terminals is presented. This method is shown to be accurate enough for comparing the performance of antenna configurations. The method enables a statistical antenna evaluation without requirements to perform long routes of radio channel sounder measurements with several antenna configurations in several environments. The results of the plane–wave based method utilizing the joint contribution of environmental data and the radiation pattern of an antenna are compared with the results of direct radio channel measurements. The average difference between the methods is below 1 dB in estimating diversity gain of two–element antennas. Further, the maximum difference between the methods in Multiple–Input Multiple–Output (MIMO) analysis is below 1 bit/s/Hz in estimating ergodic capacity.*

Keywords – *performance of mobile terminals, antenna evaluation, diversity, MIMO*

I. INTRODUCTION

In order to reach the high data rates of the next generation mobile systems, the use of multi–antenna configurations at the both ends of the radio link will be important. Mobile terminal antennas have commonly been evaluated by using the total radiated power, the total receiver sensitivity [1], or the mean effective gain (*MEG*) [1, 2, 3] as a figure of merit. The *MEG* and the equivalent isotropic radiated power have been compared in [4].

In order to obtain significant results for comparing several antenna configurations, several hundred meters of measurement routes in the several types of propagation environments are needed for each prototype antenna. This is difficult both due to the large amount of measurements needed, but also due to restrictions imposed by the authorities on the usage of the frequency bands in which commercial communications networks are operating.

It would be useful to test the performance of new multi–antenna mobile terminals in real signal propagation environments already during the early simulation phase of the design process. In this paper, we introduce and verify a new plane–wave based method for multi–antenna performance evaluation, which fulfills this requirement. The theory related to this method is presented in [5]. The method is based on previously measured radio channels and on the simulated or measured complex 3–D radiation patterns of the multi–antenna configurations under evaluation. The method is first mentioned in [6], and later applied in [7]. The approach is also used in [8] in the context of MIMO channel modeling. The presented method simplifies the evaluation process, saves evaluation time, and cuts costs. The plane–wave based method is the extension of the earlier work in which the estimation of *MEG* of single mobile terminal antennas was investigated [3].

The methods under consideration are presented in Section II. The usability of new method is evaluated in Section III. The conclusions are given in Section IV.

II. TWO ANTENNA EVALUATION METHODS

In this study, the MIMO and diversity analysis of multi–element antenna configurations are used to validate performance of the new plane–wave based method. The results of the radio channel measurement system equipped with a channel sounder, a linear transmitting (Tx) antenna array, and a spherical receiving (Rx) antenna array both employing dual–polarized patch antennas are used [9,10]. One dual polarized element consists of a vertically–polarized (VP) and a horizontally–polarized (HP) feed. On the sphere, the theta polarization is called VP and phi polarization is called HP. The Tx and Rx antenna arrays were connected to a fixed transmitter and to a moving receiver of the radio channel sounder, respectively. Fast switches were used at both ends of the link to measure all Tx and Rx channels simultaneously [10]. The measurement results of the system were used in two different ways:

A. Direct Measurement (DM)

In the direct measurement method, antenna elements are selected from the linear Tx and the spherical Rx measurement antenna arrays in order to obtain different test antenna configurations. The performance of a system can be estimated from the measured channel matrix of the selected antenna configuration [7]. The directions of main beams of the spherical antenna array elements used in the analysis are presented in Fig. 1.

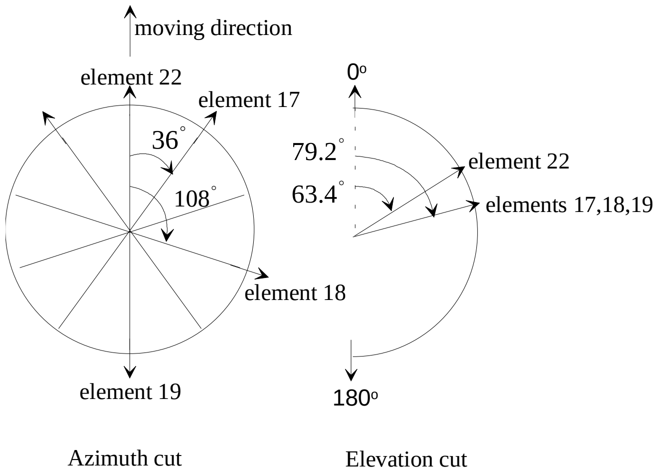

Fig. 1. The used Rx antenna elements of the spherical array

B. Plane Wave Based Method (PWBM)

The plane–wave based method is based on the joint contribution of the estimate of the distribution of radio waves and the complex 3–D radiation patterns of terminal antenna. The radiation pattern of an antenna can be written as [5]

$$\overline{E}(\Omega) = E_\theta(\Omega)\overline{a}_\theta(\Omega) + E_\phi(\Omega)\overline{a}_\phi(\Omega)\,, \qquad (1)$$

where $\overline{a}_\theta$ and $\overline{a}_\phi$ are unit vectors of spherical coordinates, E is a magnitude of the electric field, Ω is solid angle, and the subscripts θ and ϕ refer to theta and phi components of electric field. The complex 3–D radiation pattern of the antenna under test can be simulated by using software or measured in an anechoic chamber. The simulated or measured electric field of the incident plane wave can be given by

$$\overline{A}(\Omega) = A_\theta(\Omega)\overline{a}_\theta(\Omega) + A_\phi(\Omega)\overline{a}_\phi(\Omega)\,, \qquad (2)$$

where A is the magnitude of the electric field of the incident plane wave divided into two components (θ, ϕ). Finally, the complex signal envelope at the antenna port is given by

$$V(t) = \oint \overline{E}(\Omega,t)\cdot\overline{A}(\Omega,t)\,d\Omega\,, \qquad (3)$$

where t is the time parameter.

III. COMPARISON OF METHODS

Results obtained in three different propagation environments are considered: An indoor picocell environment in the Computer Science Building located in the campus area of Helsinki University of Technology (HUT), as well as outdoor microcell and small outdoor macrocell environments, both in the Helsinki downtown. The maps of the measurement routes and the plots of angle of arrival distributions of the signals are given in [7, 11].

A. Diversity Analysis

Diversity gain, which is a commonly used indicator in estimating diversity performance, is used as a figure of merit for comparing the results of the two methods. At the Tx, the VP feed of one element of the antenna array is always selected in the diversity study. At the Rx, two different antenna configurations consisting of two antennas are studied. At first, one element of the spherical antenna array consisting of a VP and a HP feed is selected. As a second option, two elements of the spherical antenna array are selected, either VP or HP feed from both the elements. In all diversity analysis, the received power is normalized according to

$$P_{i,norm} = \frac{P_{i,IN}}{\frac{1}{100}\sum_{i-50}^{i+50}\left(P_{i,Br1} + P_{i,Br2}\right)}\,, \qquad (4)$$

where $P_{i,IN}$ is the power of the branch under test, $P_{i,Br1}$ and $P_{i,Br2}$ are the powers received by the branch 1 (Br1) and the branch 2 (Br2), respectively. In the case of one dual–polarized element, Br1 and Br2 are the VP and HP feed of the element, respectively. In the case of two elements, Br1 is the element with smaller element number. In Figs. 2–4, the cumulative distribution function (cdf) of the power received by both the branches and the power after maximum ratio combining (MRC) are shown for the two compared methods.

As a first validation, measurements performed in an anechoic chamber are used to compare the two methods. In an anechoic chamber we find only one signal path, and therefore the dynamic range of a pair of orthogonal Rx elements is best visible here. The vertically polarized feed of one Tx element and the dual–polarized Rx element number 22 pointing opposite to the Tx element at 5 m distance were selected. According to the results in Fig. 2 the plane–wave based method agrees very well with the direct measurement– both in predicting the stronger branch and the 30 dB weaker branch. In Fig. 2 b) the stronger branch is magnified to show the good agreement of the two methods.

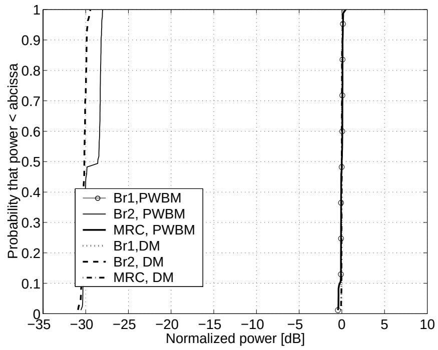

a)

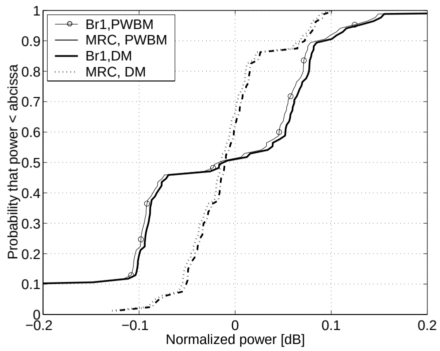

b)

Fig. 2. a) Cdf of the plane–wave based method (PWBM) and direct measurements (DM) with Rx element 22 and a vertical Tx element in an anechoic chamber. b) magnified CDFs of the stronger branch.

In order to increase the statistical significance of the comparison we define the diversity gain in two ways: the improvement achieved with the MRC is compared at first to Br1 and secondly to Br2. In Fig. 3 a) the dual–polarized antenna element 18 of the spherical antenna array was chosen to represent a polarization–diversity arrangement, the VP feed being the Br1 and HP feed being the Br2. That figure illustrates the diversity gains G_{10} and G_{50} for 10% and 50% probability levels, respectively. At 50% probability level only the weaker branch (Br2) is illustrated, and at 10% probability level only the stronger branch (Br1) is illustrated. The dotted line is used for the direct method and the solid line for the plane wave based method. In Fig. 3 b) the vertically polarized branches of two adjacent antenna elements 17 and 18 of the spherical antenna array were chosen, representing a space–diversity arrangement. Fig. 3 shows the typical examples of differing and equal power balance between the diversity branches.

In Table 1, the difference between the diversity gain values achieved with the two methods, ΔG, are given using the formula

$$\Delta G_{p,Brx} = G_{p,Brx,PWBM} - G_{p,Brx,DM} \ , \qquad [\mathrm{dB}] \qquad (5)$$

where G is the diversity gain with one method, subindex B_{rx} refers to either Br1 or Br2 and p is the probability level at which the comparison is made (p=10% or p=50%). In Table 1, Rx17 indicates that both the feeds of element 17 are used, VP feed is Br1 and HP feed is Br2. Whereas Rx1718VP indicates that Br1 is the VP feed of element 17 and Br2 is the VP feed of element 18.

According to Table 1, the average difference between the predicted and the directly measured diversity results lies within 0.87 dB for all the cases, which shows a good agreement between the two methods. In all studied cases the order of the stronger and the weaker branch are the same in both methods.

Next, we consider a more realistic mobile terminal antenna prototype. The prototype consists of two square–shaped planar inverted–F antennas (PIFA) located on the left and right upper corner of a metallic ground plane (width = 40mm, length = 100 mm). The prototype was first measured in the picocell environment mentioned before and after that, evaluated with the plane–wave based method using the simulated complex 3–D radiation patterns. Both free–space radiation patterns and radiation patterns obtained in talk position beside a phantom head model were used in the analysis. The good agreements of the cdfs in Figs. 4 a) and b) show that the plane–wave based method works well also in more realistic cases with real mobile antenna prototypes.

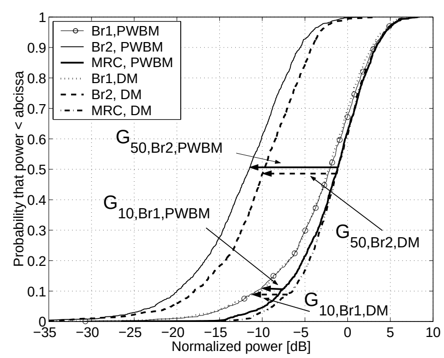

a)

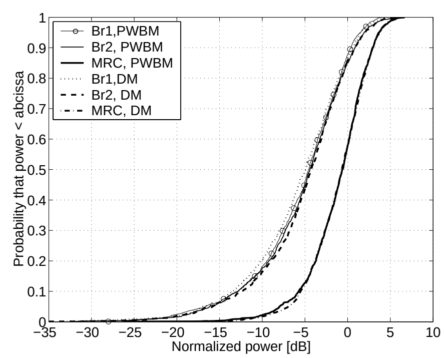

b)

Fig. 3. Comparison of the cdf of the plane–wave based method (PWBM) and direct measurements (DM) in macrocell, a) using VP and HP branches of element 18, b) using the VP branches of the elements 17 (Br1) and 18 (Br2).

Table 1. Differences in diversity gain results between the plane–wave based method and the direct method.

$\Delta G_{p,Brx}$[dB]	Br1, 10%	Br2, 10%	Br1, 50%	Br2, 50%
picocell, Rx17	-1.01	1.42	0.86	2.18
picocell, Rx1718VP	2.28	-1.04	1.91	-0.40
picocell, Rx1718HP	1.00	-1.12	1.64	-0.34
picocell, Rx18	-1.71	2.34	-0.76	2.64
picocell, Rx1819VP	0.32	0.83	-0.61	-0.44
picocell, Rx1819HP	0.09	0.83	-0.15	-0.13
picocell, Rx19	-1.70	1.90	-0.89	2.40
microcell, Rx17	-1.07	-0.33	-0.41	1.03
microcell, Rx1718VP	0.79	0.63	0.42	-0.10
microcell, Rx1718HP	-0.53	1.49	-0.28	0.68
microcell, Rx18	-1.23	2.76	-0.41	1.89
microcell, Rx1819VP	-0.02	2.18	0.06	1.06
microcell, Rx1819HP	0.03	3.90	-0.02	2.15
microcell, Rx19	-0.56	-0.27	-0.25	-0.02
macrocell, Rx17	-0.81	1.44	-1.01	0.91
macrocell, Rx1718VP	-0.79	0.21	-0.31	0.23
macrocell, Rx1718HP	-0.24	0.34	-0.21	0.53
macrocell, Rx18	-1.20	0.62	-0.18	1.73
macrocell, Rx1819VP	0.46	-1.47	0.11	-0.11
macrocell, Rx1819HP	-0.23	0.02	0.20	0.26
macrocell, Rx19	-2.11	1.70	0.23	2.14
Mean difference	-0.39	0.81	-0.11	0.87
Standard deviation	1.03	1.40	0.73	1.04

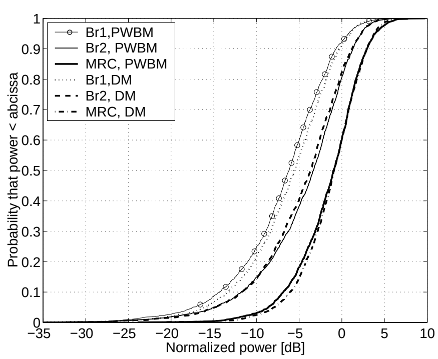

a)

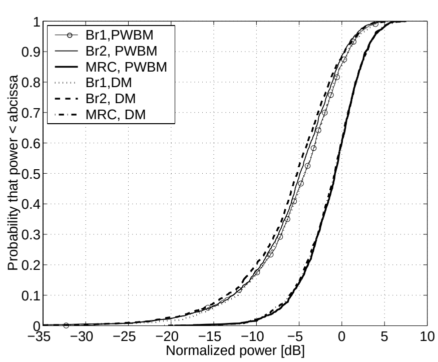

b)

Fig. 4. Comparison of the methods in picocell environment with a real mobile terminal antenna configuration a) in free space. b) beside head.

B. MIMO analysis

Shannon capacity for MIMO is defined by [12]

$$C = \log_2\left[\det\left(I + \frac{\rho}{n_t}\overline{R}_{norm}\right)\right], \quad \text{[bit/s/Hz]} \qquad (6)$$

where ρ is signal to noise ratio and I is the identity matrix. The normalized instantaneous channel correlation matrix is calculated according to [7]

$$\overline{R}_{norm} = \frac{\overline{H}^H\overline{H}}{\frac{1}{n_t n_r}E\left\{\sum_{t=1}^{n_t}\sum_{r=1}^{n_r}H^*_{r,t}H_{r,t}\right\}}, \qquad (7)$$

where $()^H$ is complex conjugate transpose, $()^*$ is complex conjugate, and $E\{\}$ is expectation operator over the sliding window. n_t and n_r are the numbers of transmitting and receiving antenna elements, respectively. $\overline{H}$ is a narrowband complex channel matrix obtained from impulse responses by at first removing noise and then using coherent summing in the delay domain.

In the MIMO analysis, the Shannon capacity and the eigenvalues of $\overline{R}_{norm}$ are used as the figures of merit. The first configuration (VPVP) includes two adjacent VP feeds from the elements at both ends of the link. The second configuration (HPVP) consists of HP and VP feeds from adjacent elements at both ends of the link. Elements 17 and 18 are selected from the spherical array (see Fig.1). The results of the configurations were normalized averaging the power over the antennas of the first MIMO system (VPVP), and in addition to this, slow fading was removed by averaging over 25λ as in diversity analysis.

The distributions (cdfs) of the instantaneous capacity (6) and of the eigenvalues of $\overline{R}_{norm}$ for both the VPVP and HPVP cases are presented in Figs. 5 and 6 in the small macrocell environment. Dotted and solid line presents the results of the direct measurement (DM) and the plane wave based method (PWBM), respectively. The best agreement between the results of the two methods is achieved with HPVP case (Fig. 6), but the relative error in the VPVP results is also insignificant (Fig. 5). The largest difference can be noticed if the weakest eigenvalue of the VPVP case is considered (in small macrocell).

The means and standard deviations of the capacity and eigenvalue results are presented in Tables 2–5 for all three investigated environments. The difference of results between the methods is evaluated by

$$\Delta X_y = X_{y,PWBM} - X_{y,DM}\ , \qquad (8)$$

where X indicates either mean (m) or variance (σ). Further, subindex y refers to either capacity (C) or eigenvalue (λ). All values are presented in linear scale.

The results of different antenna configurations are presented in separate tables. In Tables 3 and 5, the first and the second value in each cell refer to the weakest and the strongest eigenvalue, respectively.

The maximum difference in ergodic capacity (Δm_C) and standard deviation ($\Delta\sigma_C$) is 0.56 bit/s/Hz and 0.11 bit/s/Hz, respectively. The maximum difference in the mean and the standard deviation of the eigenvalues is 0.06/0.19 (Δm_λ) and 0.06/0.00 ($\Delta\sigma_\lambda$) for the weaker and stronger eigenvalues, respectively. These maximum differences presented by absolute values (see Tables 4 and 5) were found from the results of HPVP MIMO system in the picocell environment. The more extensive comparison of methods will be the subject of future study.

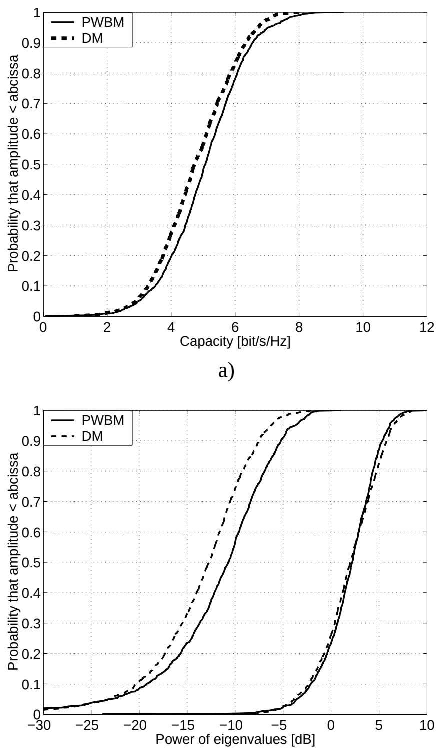

a)

b)

Fig. 5. Comparison the of methods at VPVP case. a) Capacity comparison. b) Eigenvalue comparison

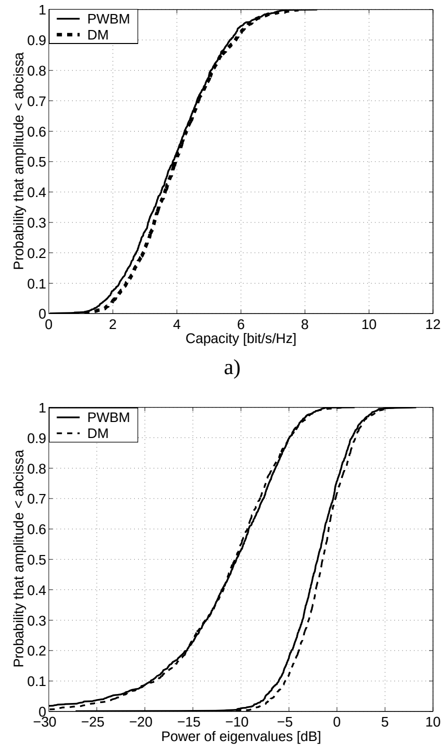

a)

b)

Fig. 6. Comparison of the methods at HPVP case. a) Capacity comparison. b) Eigenvalue comparison

Table 2. Comparison of ergodic capacity [bit/s/Hz] results of VPVP configuration

	Picocell	Microcell	Macrocell
$m_{C,\,PWBM}$	5.03	4.37	4.78
$m_{C,DM}$	4.78	4.49	5.05
Δm_C	0.25	-0.12	-0.27
$\sigma_{C,PWBM}$	1.25	1.10	1.18
$\sigma_{C,DM}$	1.22	1.12	1.24
$\Delta\sigma_C$	0.03	-0.02	-0.05

Table 3. Comparison of eigenvalue results of VPVP configuration

	Picocell	Microcell	Macrocell
$m_{\lambda,\,PWBM}$	0.13/1.84	0.04/1.87	0.08/1.95
$m_{\lambda,DM}$	0.10/1.86	0.06/1.87	0.13/1.89
Δm_λ	0.04/-0.02	-0.02/0.01	-0.05/0.06
$\sigma_{\lambda,PWBM}$	0.16/1.18	0.05/1.36	0.08/1.31
$\sigma_{\lambda,DM}$	0.14/1.24	0.08/1.35	0.14/1.17
$\Delta\sigma_\lambda$	0.02/-0.06	-0.03/0.02	-0.05/0.14

Table 4. Comparison of ergodic capacity [bit/s/Hz] results of HPVP configuration

	Picocell	Microcell	Macrocell
$m_{C,\,PWBM}$	4.54	3.57	4.04
$m_{C,DM}$	3.98	3.45	3.91
Δm_C	0.56	0.12	0.13
$\sigma_{C,PWBM}$	1.35	1.20	1.27
$\sigma_{C,DM}$	1.25	1.25	1.32
$\Delta\sigma_C$	0.11	-0.05	-0.05

Table 5. Comparison of eigenvalue results of HPVP configuration

	Picocell	Microcell	Macrocell
$m_{\lambda,\,PWBM}$	0.13/1.30	0.07/0.83	0.13/0.84
$m_{\lambda,DM}$	0.08/1.11	0.06/0.84	0.14/0.77
Δm_λ	0.06/0.19	0.01/-0.00	-0.00/0.08
$\sigma_{\lambda,PWBM}$	0.16/0.89	0.08/0.63	0.15/0.56
$\sigma_{\lambda,DM}$	0.10/0.89	0.09/0.72	0.14/0.56
$\Delta\sigma_\lambda$	0.06/0.00	-0.01/-0.09	0.01/-0.00

IV. DISCUSSION AND CONCLUSION

In this paper, the plane−wave based method was compared with direct measurements. Both the evaluation of the diversity performance of several antenna configurations and the performance of 2×2 MIMO systems were studied. The diversity gain values and relative received power estimated by the plane−wave based method agree well with the direct measurement results, and the estimation is even better in the MIMO study.

The plane−wave based method is sufficiently accurate to be used in the comparison of the performance of multi−antenna configurations. Several antenna prototypes can be studied in several propagation environments very fast by the plane−wave based method. Antennas can be rotated in azimuth and also in elevation direction easily to get comprehensive insight into the antenna characteristics which is useful e.g. in MEG analysis. Antennas can be tested already during the design process, even before a prototype antenna is constructed by using simulated radiation patterns and the previously measured channel library. Further, the radio channel stays exactly the same for all antenna configurations under test, and a virtual isotropic reference antenna, which does not distort the mean and variance results of received signals, can be used in calculations.

The limitations of the beamforming algorithm, and any other algorithm as well, in estimating details of the scattering field, is caused by the physical restrictions of the used spherical antenna array. An infinite size of array with infinite number of elements would be needed to fulfill perfect accuracy requirement. However, the spherical antenna array is the most optimal structure of antenna array in channel estimation with this given number of antenna elements [9]. In future, a more advanced channel estimation algorithm, like Space−Alternating Generalized Expectation−Maximization (SAGE) [13], could be employed in order to improve the results.

ACKNOWLEDGMENTS

We thank the following persons for their work that is related to this paper. Jarmo Kivinen developed the measurement system. Further, Kimmo Kalliola and Heikki Laitinen constructed the spherical array and implemented the beamforming algorithm.

REFERENCES

[1] G. F. Pedersen, J. O. Nielsen, “Radiation Pattern measurements of Mobile Phones next to different Head Phantoms,” in *Proc. IEEE 56th Veh. Technol. Conf. (fall)*, vol. 4, 2002, pp. 2465−2469.

[2] T. Taga, “Analysis for Mean Effective Gain of Mobile Antennas in Land Mobile Radio Environments,” *IEEE Trans. Veh. Technol.*, vol. 39, pp. 117−131, May 1990.

[3] K. Sulonen, P. Vainikainen, “Performance of Mobile Phone Antennas Including Effect of Environment Using Two Methods,” *IEEE Trans. Instrum. Meas.*, vol. 52, pp.1859−1864, Dec. 2003.

[4] M. B. Knudsen, G. F. Pedersen, B. G. H. Olsson, K. Olesen, S. A. Larsson, “Validation of Handset Antenna Test Methods,” *IEEE Proc. 52th Veh. Technol. Conf. (fall)*, 2000, pp. 1669−1676.

[5] Y. S. Yeh, “Antennas and Polarization Effects”, Chapter 3 in *Microwave Mobile Communications,* editor W. C. Jakes, New York, Wiley, 1974, 642 p.

[6] J. Kivinen, P. Suvikunnas, L. Vuokko, P. Vainikainen, “Experimental investigations of MIMO propagation channels”, *in Proc. IEEE Int. Symp. Antennas and Propagation*, 2002, pp. 16−21.

[7] K. Sulonen, P. Suvikunnas, L. Vuokko, J. Kivinen, and P. Vainikainen, “Comparison of MIMO Antenna Configurations in Picocell and Microcell Environments,” *IEEE J. Select. Areas Commun.*, vol. 21, 2003, pp.703−712.

[8] H. Xu, D. Chizhik, R. Valenzuela, “Wave based wideband MIMO channel modeling technique”, in *Proc. the 13th IEEE International Symposium on Personal, Indoor and Mobile Radio Communications*, vol. 4, 2002, pp. 1626−1630.

[9] K. Kalliola, H. Laitinen, L. Vaskelainen, and P. Vainikainen, “Real−time 3−D spatial−temporal dual−polarized measurement of wideband radio channel at mobile station,” *IEEE Trans. Instrum. Meas.*, vol. 49, pp. 439−448, April 2000.

[10] J. Kivinen, P. Suvikunnas, D. Perez, C. Herrero, K. Kalliola, P. Vainikainen, “Characterization system for MIMO channels,” in *Proc. 4th Int. Symp. Wireless Personal Multimedia Communications*, 2001, pp. 159−162.

[11] K. Sulonen, P. Suvikunnas, J. Kivinen, L. Vuokko, P. Vainikainen, “Study of different mechanisms providing gain in MIMO systems,” in *Proc. IEEE 58th Veh. Technol. Conf. (fall),* 2003, paper 03C_01.pdf

[12] G. J. Foschini, “Layered space−time architecture for wireless communication in a fading environment when using multi-element antennas,” *Bell Labs Technical Journal*, pp. 41−59, 1996.

[13] K. I. Pedersen, B. H. Fleury, P. E. Mogensen, “High Resolution of Electromagnetic Waves in Time−Varying Radio Channels,” in *Proc. the 8th IEEE International Symposium on Personal, Indoor and Mobile Radio Communications*, 1997, pp. 650−654.